# Optical hop number limits imposed by various $2 \times 2$ cross-connect node designs

**Edward Mutafungwa**
*Communications Laboratory, Otakaari 8 (PL 2300), Helsinki University of Technology, FIN-02015 HUT, Finland*
*edward.mutafungwa@hut.fi*

**Abstract:** The success of transparent optical transport networks depends on the availability of optical cross-connect nodes (OXNs) that induce minimal impairments on the signals they cross-connect. This should extend the possible coverage and flexibility of path restoration within a meshed network topology by raising the upper bound on the achievable optical hop (traversable OXNs) number. We provide a brief survey and categorization of the currently proposed OXNs. Furthermore, the possible limits they impose on the number of hops are established by a series of transmission performance simulations. Microoptic and all-fiber OXNs are identified to be suitable for networks with a low connectivity and channel count. In case larger OXNs are needed, then microoptic and integrated OXNs provide a better option. The results obtained are applicable as guidelines for the deployment of future optical ring topologies.



**OCIS codes:** (060.4510) Optical communications (060.4250) Networks

## References and links

1. H. Yoshimura, K. I. Sato and N. Takachio, "Future photonic transport networks based on WDM technologies," IEEE Commun. Mag. **37**, 74-81 (1999).
2. T. Stern and K. Bala, "Multiwavelength optical networks: A layered approach," Addisson-Wesley, Reading (1999).
3. E. L. Goldstein, L. Y. Lin and R. W. Tkach, "Multiwavelength opaque optical-crossconnect networks," IEICE Trans. Electron **E82-C**, 1361-1370 (1999).
4. E. Iannone and R. Sabella, "Optical path technologies: A comparison among different crossconnect architectures", J. Lightwave Tech.**14**, 2184-2196 (1996).
5. N. A. Jackman, S. H. Patel, B. P. Mikkelsen and S. K. Korotky, "Optical cross connects for optical networking," Bell Labs Technol. J. **4**, 246-261 (1999).
6. B. Ramamurthy, D. Datta, H. Feng, J. P. Heritage and B. Murkherjee, "Impact of transmission impairments on the teletraffic performance of wavelength-routed optical networks," J. Lightwave Tech.**17**, 1713-1723 (1999).
7. G. Wilfong, B. Mikkelsen, C. Doerr and M. Zirngibl, "WDM cross-connect architectures with reduced complexity," J. Lightwave Tech. **17**, 1732-1741 (1999).
8. S. Chandrasekhar, H. K. Kim, C. R. Doerr, L. W. Stulz and L. L. Buhl, "All-optical dual ring internetworking with wavelength selective $2 \times 2$ cross-connect," Electron. Lett. **36**, 238-239 (2000).
9. S. Baroni, P. Bayvel, R. J. Gibbons and S. K. Korotky, "Analysis and design of resilient multifiber wavelength-routed optical transport networks," J. Lightwave Tech.**17**, 743-758 (1999).
10. M. Sinclair, "Minimum cost wavelength-path routing and wavelength allocation using a genetic-algorithm/heuristic hybrid approach," IEE Proc. Commun. **146**, 1-7 (1999).
11. R. Sabella, E. Iannone, M. Listanti, M. Berdusco and S. Binetti, "Impact of transmission performance on path routing in all-optical transport networks," J. Lightwave Tech.**16**, 1965-1972 (1998).
12. D. Tanis, "Carriers can maximize their dark-fiber returns," FiberSystems Europe **5**, 41-44 (2001).
13. E. Pennings, G. D. Khoe, M. K. Smit and T. Staring, "Integrated-optic versus microoptic devices for fiber-optic telecommunications systems: A comparison," IEEE J. Select. Topics Quantum Electron. **2**, 151-164 (1996).
14. A. Himeno, K. Kato and T. Miya, "Silicon-based planar lightwave circuits," IEEE J. Select. Topics Quantum Electron. **4**, 913-924 (1998).
15. S. Charbonneau, E. S. Koteles, P. J. Poole, J. J. He, G. C. Aers, J. Haysom, M. Buchanan, Y. Feng, A. Delage, F. Yang, M. Davies, R. D. Goldberg, P. G. Piva and I. V. Mitchell, "Photonic integrated circuits fabricated using ion implantation," IEEE J. Select. Topics Quantum Electron. **4**, 772-793 (1998).
16. K. O. Hill and G. Meltz, "Fiber Bragg grating technology fundamentals and overview," J. Lightwave Tech. **15**, 1263-1276 (1997).

#35114 - $15.00 US Received August 29, 2001; Revised September 28, 2001

17. H. G. Limberger, A. Iocco, R.P. Salathe, L. A. Everall, K. E. Chisholm and I. Bennion, "Wideband tunable fibre Bragg grating filters," Proc. 25th European Conf. Optic. Commun. **1**, 156-159 (1999).
18. H. Nakajima, "Development on guided-wave switch arrays," IEICE Trans. Electron. **E82-C**, 1263-1276 (1997).
19. K. McGreer, "Arrayed waveguide for wavelength routing," IEEE Commun. Mag. **36**, 62-68 (1998).
20. C. G. P. Herben, D. H. P. Maat, X. J. M. Leijtens, M. R. Leys, Y. S. Oei and M. K. Smit, "Polarization independent dilated WDM cross-connect on InP," IEEE Photon. Techn. Lett. **11**, 1599-1601 (1999).
21. D. A. Smith, A. D'Alessandro, J. E. Baran, D. J. Fritz, J. L. Jackel and R. S. Chakravarthy, "Multiwavelength performance of an apodized acoustic-optic switch," J. Lightwave Tech. **14**, 2044-2051 (1996).
22. M Janson, L. Lundgren, A. -C. Mörner, M. Rask, B. Stoltz, M. Gustavsson and L. Thylen, "Monolithically integrated 2×2 {InGaAs/InP} laser amplifier gate switch arrays," Electron. Lett. **28**, 776-778 (1992).
23. A. Watanabe, S. Okamoto and K. I. Sato, "Optical path cross-connect system architecture suitable for large scale expansion," J. Lightwave Tech. **14**, 2162-2172 (1996).
24. K. -H. Kim, S. -W. Kwon, J. -W. Park, S. -B. Lee and S. -S. Choi, "A new all-fiber bidirectional optical cross-connect with tunable fiber Bragg gratings," Tech. Digest Optic. Commun. Conf. **1**, 261-263 (1999).
25. S. -K Park, J. -W. Park, S. -R. Lee, H. Yoon, S. -B. Lee and S. -S. Cho Multiwavelength Bidirectional Optical Crossconnect Using Fiber {B}ragg Gratings and Polarization Beam Splitter," IEEE Photon. Techn. Lett. **10**, 531-533 (1998).
26. D. Hjelme, H. Storoy and J. Skaar, "Reconfigurable all-fiber all-optical cross-connect node using synthesized fiber Bragg gratings for both demultiplexing and switching," Tech. Digest Optic. Commun. Conf. **1**, 65-66 (1998).
27. Y. K. Chen and C. C. Lee, "Fiber Bragg grating-based large nonblocking multiwavelength cross-connects," J. Lightwave Tech. **16**, 1746-1756 (1998).
28. C. Marxer and N. F. de Rooij, "Micro-opto-mechanical 2×2 switch for single-mode fiber based on plasma-etched silicon mirror and electrostatic actuation," J. Lightwave Tech. **17**, 2-6 (1999).
29. J. Skinner and C. H. R. Lane, "A low crosstalk microoptic liquid crystal switch," IEEE J. Select. Areas Commun. **6**, 1178-1185 (1998).
30. R. Laughlin and T. Hazelton, "Frustrated total internal reflection an alternative for optical cross-connect architecture," Proc. 11th IEEE/LEOS Annual Meeting. **2**, 171-172 (1998).
31. J. E. Fouquet, "Compact optical cross-connect switch based on total internal reflection in a fluid-containing planar lighwave circuit," Tech. Digest Optic. Commun. Conf. **1**, TuM1-1 (2000).
32. J. L. Jackel, J. J. Johnson and W. J. Tomlinson, "Bistable optical switching using electromagnetically generating bubbles," Optics Lett. **15**, 1470-1472 (1990).
33. M. Sato, M. Makihara, F. Shimokawa and Y. Nishida, "Self-latching waveguide optical switch basd on thermo-capillarity," Proc. 23rd European Conf. Optic. Commun. **2**, 73-76 (1997).
34. N. Riza, "High-optical-isolation low-loss moderate-switching-speed nemetic liquid-crystal optical switch," Optics Lett. **19**, 1780-1782 (1994).
35. J. Kim, J. Jung, S. Kim and B. Lee, "Reconfigurable optical cross-connect using WDM MUX/DEMUX pair and tunable fibre Bragg gratings," Electron. Lett. **36**, 1470-1472 (1990).
36. T. A. Birks, D. O. Culverhouse, S. G. Farwell and P. S. J. Russell, "2×2 single-mode fiber routing switch," Optics Lett. **10**, 722-724 (1996).
37. A. E. Fatatry, S. P. Shipley and R. Tyson, "4×4 all-fiber optical switching matrix," Electron. Lett. **24**, 339-340 (1996).
38. S. Nagaoka, "Compact latching-type single-mode-fiber switches fabricated by a fiber-micromachining technique and their practical applications," IEEE J. Select. Topics Quantum Electron. **5**, 36-45 (1999).
39. A. Lowery, O. Lenzmann, I. Koltchanov, R. Moosburger, R. Freund, A. Richter, S. Georgi, D. Breuer and H. Hamster, "Multiple Signal Respresentation Simulation of Photonic Devices, System and Networks," IEEE J. Select. Topics Quantum Electron. **6**, 282-296 (2000).
40. E. Mutafungwa, "Circulating loop simulations for transmission performance comparison of various node architectures," J. Opt. A: Pure Appl. Opt. **3**, 255-261 (2001).
41. D. H. P. Maat, Y. C. Zhu, F. H. Groen, H. van Brug, H. J. Frankena and X. J. M. Leijtens Polarization-independent dilated InP-based space switch with low crosstalk," IEEE Photon. Technol. Lett. **12**, 284-286 (2000).
42. Y. Pan, C. Qiao and Y. Yang, "Optical mulstistage interconnection networks: New chanllenges and approaches," IEEE Commun. Mag. **37**, 50-56 (1999).
43. R. Kasahara, M. Yanagisawa, A. Sugita, T. Goh, M. Yasu, A. Himeno and S. Matsui, "Low-power consumption silica-based 2×2 thermooptic switch using trenched silicon substrate," IEEE Photon. Technol. Lett. **11**, 1132-1134 (1999).
44. A. Kaneko, A. Sugita and K. Okamoto, "Recent progress on arrayed waveguide gratings for DWDM applications," IEICE Trans. Electron. **E83-C**, 860-868 (2000).
45. A. Carballer, M. A. Muriel and J. Azana, "Fiber grating filter for WDM systems: An improved design," IEEE Photon. Technol. Lett. **11**, 694-696 (1999).
46. N. Goto and Y. Miyazaki, "Wavelength-division-multiplexing photonic switching system using integrated acoustooptic switches," Japan. J. Appl. Phy.: Part 1 **39**, 3078-3082 (2000).
47. D. O. Culverhouse, R. I. Laming, S. G. Farwell, T. A. Birks and M. N. Zervas, "All Fiber 2×2 Polarization Insensitive Switch," IEEE Photon. Technol. Lett. **9**, 455-457 (1997).

#35114 - $15.00 US Received August 29, 2001; Revised September 28, 2001

48. E. Ciaramella, "Introducing wavelength granularity to reduce the complexity of optical cross-connects," IEEE Photon. Technol. Lett. **12**, 699-701 (2000).

## 1. Introduction

The future vision of optical transport networks is of a communication system capable of providing an optical-domain-based, format-independent grooming, routing and management of signals with distinct center frequencies (wavelengths) based on dense wavelength division multiplexing (DWDM) transmission [1]. Among the benefits expected from such an implementation is the increased capacity utilization of the underlying fiber infrastructure and the improved flexibility of multiservice provisioning by network operators. This has motivated the development of standardized networking solutions based on the same principle. The notable examples being the Automatic Switched Optical Network (ASON) and Generalized Multi-Protocol Label Switching (GMPLS) by the International Telecommunications Union (ITU) and Internet Engineering Task Force (IETF) respectively. Crucial to the success of these optical networking proposals is the deployment of intelligent wavelength-selective optical cross connect nodes (OXNs) in the current incongruous networks [1, 2 Chapt. 4]. These OXNs introduce wavelength reconfigurability to the network thus creating the possibility of delivering bandwidth-on-demand, bandwidth trading, alleviation of network congestion and the non-disruptive scaling of the network. Moreover, wavelength-level management is also possible for monitoring the quality-of-service (QoS) integrity of existing connections and the rapid service restoration in the event of a fault in the network.

To achieve some of the goals outlined above, suggestions have been made [3] for opaque optical networks that interrupt an optical signal's progress along a path by applying periodic optical-to-electrical and electrical-to-optical (OEO) conversions. This enables operations such as fault isolation, performance monitoring, wavelength translation and 2R signal regeneration (using transponders as shown in Figure 1). Indeed, these operations can be easily carried out using commercially available electronic devices---akin to current SDH/SONET systems---instead of optical components that are yet to achieve the maturity necessary for field applications. However, the introduction these opaque network elements translates into an increase in network deployment or upgrade costs, creation of bandwidth bottlenecks, accumulation of timing jitter and loss of flexibility in scaling the signal data rates.

#35114 - $15.00 US Received August 29, 2001; Revised September 28, 2001

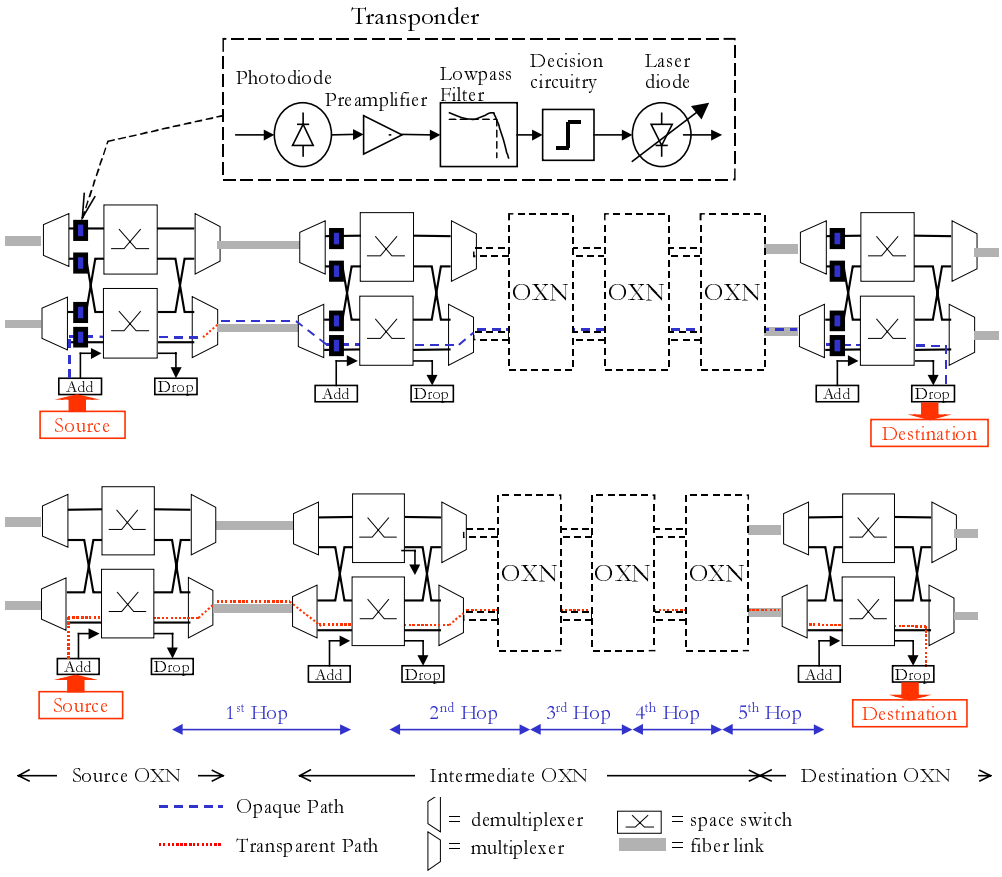


Fig.1. Excerpts of an (top) opaque optical network consisting of OXNs with in-built transponders and (bottom) transparent network with 5 optical hop path.

It is therefore of great interest (from the network operator's point of view) to deploy OXNs, setting up transparent signal paths that are uninterrupted by OEO conversions as depicted in Figure 1. This depends on the availability of OXNs that are composed of feasible subsystems (building blocks) and impart insignificant impairments (e.g., attenuation, distortion, noise etc.) on the signals they cross-connect. The latter condition should enable a signal to traverse a large enough number of OXNs before any reshaping and re-timing of the signal becomes necessary. As a result, the upper limit on the number of optical hops (that is, traversable OXNs in the absence of transponders) *H* could be kept at a level that renders feasibility to all the paths ordered by the network's routing algorithms. A wide range of OXNs has been reported (see [4, 5] and references quoted therein), each one of them imposes their own limits on *H* depending on their architectural configurations and the extent to which they contribute to signal's degradation [6].

In this paper, we analyze the apparent limitation on *H* imposed by various fundamental or **2×2** (two input/output fiber port) OXNs. The reason being that the fundamental OXNs can be used as integral parts of a larger OXN [7] or as optical add-drop multiplexers (OADMs) in DWDM shared-protection rings (SPRINGs) [8]. Optical network architectures and wavelength routing techniques are reviewed briefly in Section 2. Various reported OXNs are summarized in Section 3 and an OXN categorization is proposed so as to ease their comparison. Section 4 describes the simulation and comparison of the transmission performance of different OXN designs.

#35114 - $15.00 US
Received August 29, 2001; Revised September 28, 2001

## 2. Practical Network Topologies

The transition from current legacy networks to an all-encompassing optical network is dependent on the fulfillment of the following obligations: fault tolerance [9], efficient resource allocation [10] and improved transmission performance [6, 11]. This points towards a need for an underlying physical meshed topology with the following favorable attributes [2, Chapt. 6]:

- Small diameter, that is, the maximum number of minimum hops between any node pair.
- Low overall mean hop number attained by maximizing physical connectivity or convergence towards the Moore bound.
- Upper limits on the node degree (incoming/outgoing links), thus reducing the complexity of the network switch designs.
- Planar (with no links crossing one another) layout with a high degree of symmetry, enabling centralized control and simplifying network planning, scaling, fault recovery and expedition of dynamic resource allocation.

However, the physical topologies of most practical optical networks deviate significantly from these characteristics due to the semirandom and piecemeal deployment of the networks. This is attributed to the need to match the deployment process with the traffic growth trends of a particular service area, thus guaranteeing returns on the investment in fiber plant and terminal equipment. Indeed, this randomness can also be seen in the flourishing dark fiber leasing (or swapping) transactions between various incumbent operators and new entrants, as they cautiously increase their network coverage and capacity [12].

For the case of wavelength routing, routing and wavelength assignment (RWA) algorithms generate a finite number of paths and dispense wavelength channels in response to incoming connection requests [10]. In these RWA routines, the shortest path is requested when setting up a connection between any source-destination node pair so as to minimize signal degradation, delay and wastage of network resources. The length of the path is quantified in terms of performance-critical parameters such as geographical distance, optical hops $H$ or link loading. Since the focus of this paper is principally on optical hop constraints, then the path length is considered to be the $H$.

In the event of failure to any of the operational links or nodes within the network, alarm indication signals are generated and appropriate service restoration procedures are initiated by the network management system. The latter restores the service or connection by instructing the nodes affected by the failure to resume the connection on a pre-selected or recalculated node- or link-disjoint restoration path [9]. In majority of the cases, the restoration path would have a larger $H$ compared to the original working path and is therefore more susceptible to the build-up of OXN penalties.

## 3. Classification of OXNs

The various OXN architectures can be classified according to their blocking characteristics (strictly non-blocking, rearrangably non-blocking or blocking [4,7]), routing strategies (wavelength-selective or wavelength-interchanging [2, Chapt. 2]) or inherent modularity (link and/or wavelength modular [4]). We adopt the categories proposed by Pennings *et al* [13], hence, classifying the OXNs according to the design technology of their subsystems. Therefore, the four main OXN categories are:

1. *Integrated-Optic OXNs*: Implemented using photonic integrated circuits (PICs) that reduce the optical interconnection costs of guided-wave OXN subsystems. This produces compact OXNs with miniaturized components that can—in some special cases—be co-located on a single chip (substrate). Silicon (Si) is one of the widely used substrates [14], whereby optical signals are transported by silica waveguides etched on the Si substrate. Current examples include star couplers, Mach-Zehnder interferometric (MZI) thermo-optic switches, phase-shifters and arrayed-waveguide gratings (AWGs). It also possible to fabricate components by diffusing higher index waveguides on alternative electro-optic

#35114 - $15.00 US Received August 29, 2001; Revised September 28, 2001

dielectric or III-V substrates, such as lithium niobate ($LiNbO_3$) or indium phosphide (InP) [15].

2. *All-Fiber OXNs*: Utilizing components made from specialty fibers made by fusing, doping or radiating fiber waveguides. This enables them to perform functions in addition to the low-loss transfer of signals between two points. An obvious example is the erbium-doped fibers used for optical amplification [1]. Another specialty fiber that is gaining prominence in the field of optical networking is the fiber Bragg grating (FBG) [16]. They are made by inscribing gratings (index variations) on the core of the fiber using ultraviolet radiation, the grating period dictating the wavelength of the signal(s) reflected back by the FBG. Furthermore, the grating period can be varied by applying temperature variations, mechanical strain or magnetic-actuation, thus making the FBGs wavelength tunable [17].
3. *Microoptic OXNs*: Constitutes stand-alone or combined components that relay an optical beam by collimating, reflecting, shaping or diffracting the beam. The part of the component that interacts with the beam is made of materials in the form of solids (e.g., mirrors, glass prisms etc.), liquids (e.g., index matching oil etc.) or liquid crystals (oriented like crystals but with chaotic positional order like liquids).
4. *Hybrid OXNs*: Made up of a combination of component technologies from the previous three categories.

A more specific listing of the proposed OXNs for each of the above categories is presented in Table 1. The OXNs H3-H5 are considered to be hybrid since it is assumed that they use non-fiber based multiplexers/demultiplexers. All the entries marked with an asterisk mean that the OXN has configuration different from the multiplexer-switch-demultiplexer configuration of Figure 1.

#35114 - $15.00 US Received August 29, 2001; Revised September 28, 2001

Table 1. The list of OXNs considered in the study

| Category | Distinguishing Features | Alias | Ref. |
|---|---|---|---|
| Integrated | Titanium diffused $LiNbO_3$ electro-optic switches | I1 | [18] |
| | AWGs & MZI thermo-optic switches on Si | 12 | [19] |
| | AWG & dilated MZI electro-optic switches on InP | 13 | [20] |
| | Acousto-optic switch with proton-exchanged waveguides on $LiNbO_3$ | 14 | [21] |
| | Semiconductor optical amplifier gate switch matrix on InGaAsP/InP | 15 | [22] |
| | Delivery/coupling constituting gating 1×2 MZI switches on Si | 16 | [23] |
| All-Fiber | Passive fiber splitters/combiners and FBGs | F1 | [24] |
| | FBGs, polarization beam splitter (PBS) pair and quater wave plates | F2 | [25] |
| | FBGs, 3-port optical circulators (OCs) and passive combiners | F3 | [26] |
| | FBGs and OCs | F4 | [27] |
| Microoptic | Switching by micro electro-mechanical systems (MEMS) erected on Si | M1 | [28] |
| | Switching by a liquid crystal in between movable glass prisms | M2 | [29] |
| | Bulk optics based frustrated total internal reflection (FTIR) switches | M3 | [30] |
| | Switching using bubbles generated by a thermal actuator | M4 | [31] |
| | Switching using $O_2$ or $H_2$ bubbles generated by electrolysis of water} | M5 | [32] |
| | Switching implemented by oil displaced thermal-capillarity forces | M6 | [33] |
| | Switch made of PBSs and liquid crystals | M7 | [34] |
| Hybrid | FBGs and an AWG pair | H1 | [35] |
| | FBGs, OCs and opto-mechanical switches | H2 | [27] |
| | Acousto-Optic fiber switch based on asymmetric fiber couplers | H3 | [36] |
| | Fiber MZI switch with a thermal or mechanical phase shifter | H4 | [37] |
| | Latching-type fiber switches using micromachining techniques | H5 | [38] |

## 4. Performance Analysis

Simulations are carried out using the photonic transmission design suite (PTDS version 1.3 by Virtual Photonics Inc.) running on a Windows™ NT platform [39]. Within PTDS the components that make up the OXN subsystems are imitated by custom or user-defined modules based on their individual numerical models. Optical and electrical signals are represented as computer data that is exchanged between interconnected modules via a simulation environment adaptation layer. The response of a module to input signals is obtained by evaluating their numerical models (written as basic C++ code) in the optical network simulation layer.

### *4.1 Simulation Configuration*

A setup was created to compare the transmission performance of OXNs in a 4×2.5 Gbit/s WDM system using the intensity modulated-direct detection (IM/DD) scheme and $2^{15}$–1 pseudo-random word patterns. The 4 channels $f_1$–$f_4$ spanning 192.95-193.25 THz are spaced at 100 GHz and. The simulation configuration (see Figure 2) comprises a 35 km optical re-circulating loop with the 2×2 OXN under test, a singlemode fiber (SMF) fiber link and a spool

#35114 - $15.00 US Received August 29, 2001; Revised September 28, 2001

of dispersion compensating fiber (DCF). This particular re-circulating loop configuration offers a significant reduction in computation times in comparison to simulation of an entire network [40].

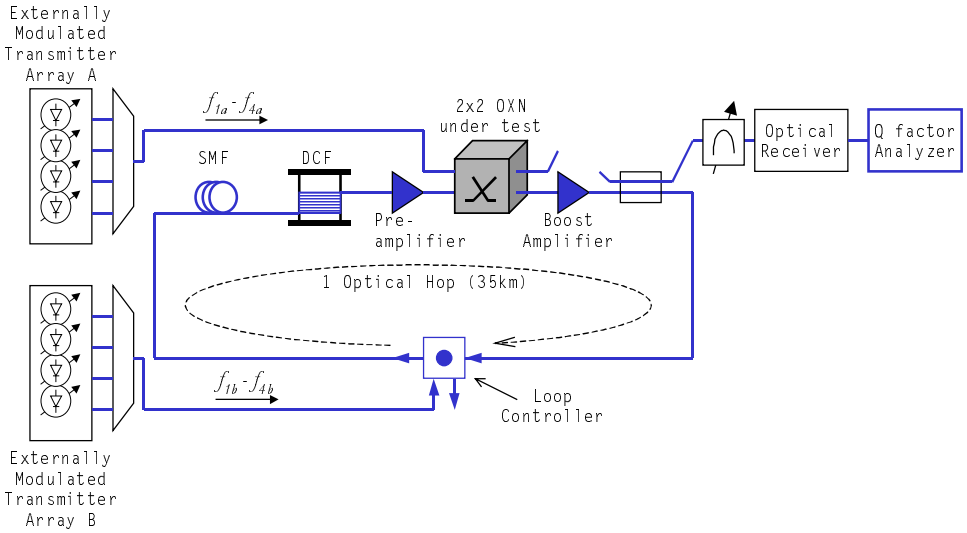


Fig. 2. Simulation configuration of OXN circulating loop captured in PTDS simulation environment.

In the above setup, all the intermediate OXNs have been configured to swap channels $f_1$, $f_3$ between the two incoming fibers whilst passing through channels $f_2$, $f_4$. Therefore, $f_2$ and $f_4$ traverse all the intermediate nodes whose total count is equivalent to number of re-circulation loop cycles (=$H$). The signal quality of $f_{2b}$ or $f_{4b}$ at the OXN output is analyzed after every loop cycle so as to monitor the QoS degradation at the end of each hop.

### *4.2 Modules and Simulation Parameters*

An OXN is created by a synthesis of PTDS modules with adjustable parameters or if unavailable, user-defined modules tailored to approximate the behavior of a novel optical device. The modules used in the simulation and their respective parameters are shown in Table 2.

Table 2. The main modules and parameter values used in the simulations.

| Modules | Parameter/Settings |
|---|---|
| Transmitter | Ext. Modulated; 1.0 mW Av. power; 10 MHz Linewidth; 30 dB Extinction ratio |
| Pre-amplifier | Gain controlled mode; 9.2 dB Gain; 4 dB Noise figure |
| Boost Amplifier | Power controlled mode; -6.0dBm/channel output; 3.5 dB Noise figure |
| SMF (G.652) | 0.2 dB/km Attenuation; 16 ps/nm-km Dispersion; $2.6\times10^{-20}$ $m^2/W$ Nonlinearity coefficient |
| DCF (G.653) | 0.6 dB/km Attenuation; -90 ps/nm-km Dispersion; $4.0\times10^{-20}$ $m^2/W$ Nonlinearity coefficient |
| Receiver | PIN detector; 1 A/W Responsivity; $10^{-12}A\sqrt{Hz}$ Thermal noise; Bessel Filter 1.75 MHz cutoff |

#35114 - $15.00 US
Received August 29, 2001; Revised September 28, 2001

After a particular simulation run the system performance is established by numerically evaluating the *Q* factor (electrical signal-to-noise ratio) using a Gaussian approximation method with an optimum threshold setting and a module for ideal clock recovery. Assuming that $I_i$ and $\sigma_i$ represent the photocurrent and noise variance respectively for a received bit $i \in \{0,1\}$, the *Q* factor is given by [11]

$$Q = \frac{|I_1 - I_0|}{\sigma_1 + \sigma_0}, \tag{1}$$

and is related to the bit error rate (BER) by

$$BER = \frac{\exp(-Q^2/2)}{Q\sqrt{2\pi}}. \tag{2}$$

The *Q* factor can also be expressed in dB by *Q factor* dB = 20log(Q).

*4.3 Internal OXN Components*

The OXNs considered here make use of a diverse range of technologies. We quote the parameters used in the design, testing and experimental demonstration of the OXNs, directly from their respective references listed in Table 1. Subsequent improvements in various OXN subsystems due to improved component designs are also considered so as to give a more up-to date status on the OXN transmission performance. These updated state-of-the-art designs include:

- Space division switches based on a dilated Benes network using four 2×2 switching elements to form a single 2×2 switch. Using this technique, the isolation of MZI (on InP) and Ti:$LiNbO_3$ switches was improved by 20 dB [41] and 10 [42] respectively.
- Power consumption of MZI thermo-optic switches on Si reduced by over two thirds of previous designs without any increase in losses or extinction ratio [43].
- All AWGs on Si are assumed to be adjusted to provide polarization independence and improved crosstalk isolation (<–40 dB) for a 100 GHz channel spacing [44].
- All FBGs considered have an optimum apodized index change (55 dB isolation for 100 GHz spacing) and are designed in a two stage process that eliminates resonance occurring at the short-wavelength side of grating [45].
- Modified design of integrated acousto-optic switches that maintain the switched signal's polarization and eliminates the need for anisotropy for the waveguide material [46].
- The polarization dependent loss of fiber acoustic optic switches made negligible (reduced by over 15 dB) by twisting the waist of the asymmetric coupler [47].

Unless stated otherwise in Table 1, the $N \times 1$ wavelength multiplexers are implemented using a total of *N* third order Bessel bandpass filters with distinct center frequencies, a default 3.0 dB insertion loss and passband of 40 GHz. The demultiplexers are also implemented using Bessel filters with similar specifications.

**5. Simulation Results**

The quality (*Q factor*) of $f_{2b}$ after every subsequent hop via intermediate integrated (I1-I6) OXNs is shown in Figure 4a. Also included is *Q factor* for the same signal if no intermediate OXNs were present on the path (that is, if OXNs are perfectly ideal) thus only highlighting the signal degradations attributed to components outside the OXNs (mainly fiber impairments). In this case the boost amplifiers are not used and the preamplifiers are considered to be in-line amplifiers (1R repeaters). Additional results for all-fiber (F1-F4), microoptic (M1-M7) and hybrid (H1-H5) intermediate OXNs are depicted in Figures 4b to d respectively.

#35114 - $15.00 US Received August 29, 2001; Revised September 28, 2001

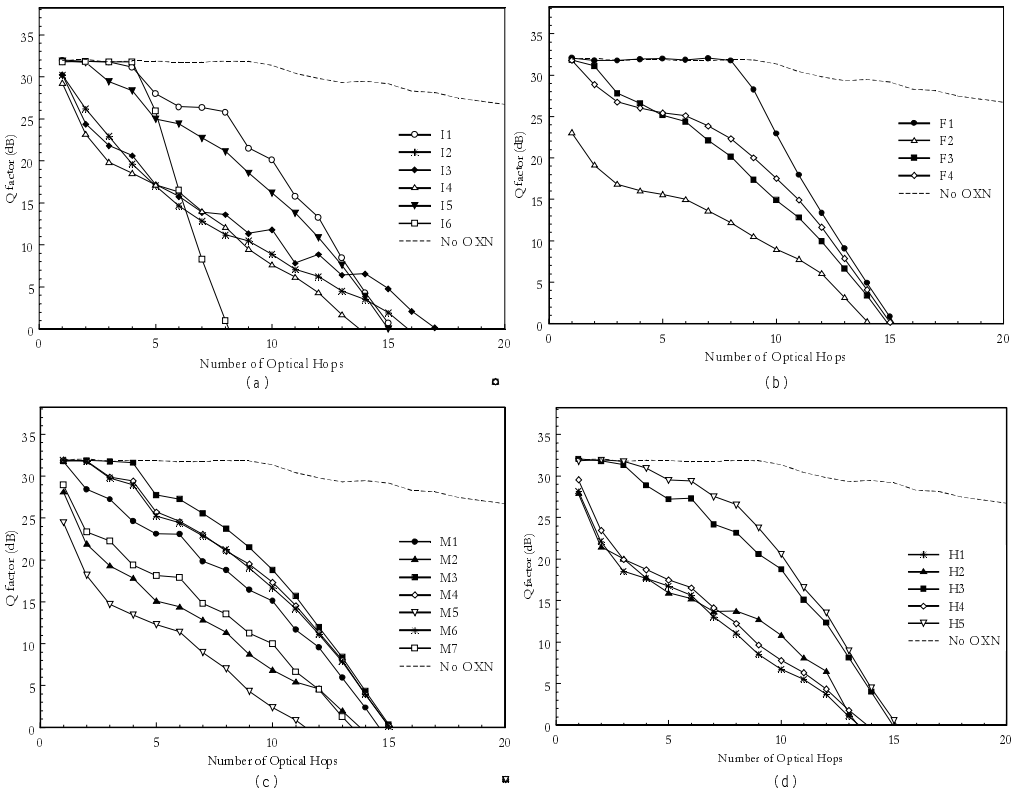


Fig. 4. Simulated *Q factor* of the $f_{2b}$ signal and received via various (a) integrated (b) all-fiber (c) microoptic and (d) hybrid OXNs.

The best transmission performance attained in all cases (I1, F1, M3, and H5) is noted for OXNs that characterized by near ideal (specifically low loss and high crosstalk isolation) subsystems. Improvements in the isolation of InP-based MZI switches have meant that I5 is among the best performing integrated switch. All-fibers OXNs generally offer a satisfactory hop reach, unless they are compromised by components whose performance is far from ideal, such as the fiber PBSs used in F2 (see Figure 4b). Similar observations can be made for hybrid OXNs that makes use of both near ideal (FBGs) and far from ideal (opto-mechanical switches), as in H2 (see Figure 4d). However, alternative hybrid OXNs made of all-fiber switching techniques that do not involve FBGs (H3, H5) display adequate transmission performance. The microoptic OXNs based on novel switching techniques (M1, M3, M4, and M6) consistently outperform some of the earlier proposed designs (M2, M7) as depicted in Figure 4c.

Assuming that connections are automatically dropped or blocked if *Q factor* = 15 dB (corresponding to a BER $10^{-9}$), the plot of Figure 5 indicates the number of achievable optical hops (i.e., traversable OXNs) for each 2×2 OXN type. All-fiber and microoptic demonstrate on average the best cascadability. However the alternative configuration of the former is such that their transmission performance deteriorates rapidly when the number of channels $N_\lambda$ or node degree $\Delta$ is increased. This is due to fact the number components OXN is also increased to accommodate the extra channels or fiber ports and each component is viewed as a potential cause of signal impairment. For instance, when $N_\lambda$ is increased from 4 to 80, an F3 2×2 OXN

#35114 - $15.00 US Received August 29, 2001; Revised September 28, 2001

will need an additional 690 components to cross-connect the added channels. An M1 OXN of similar dimensions will only need 80 more components.

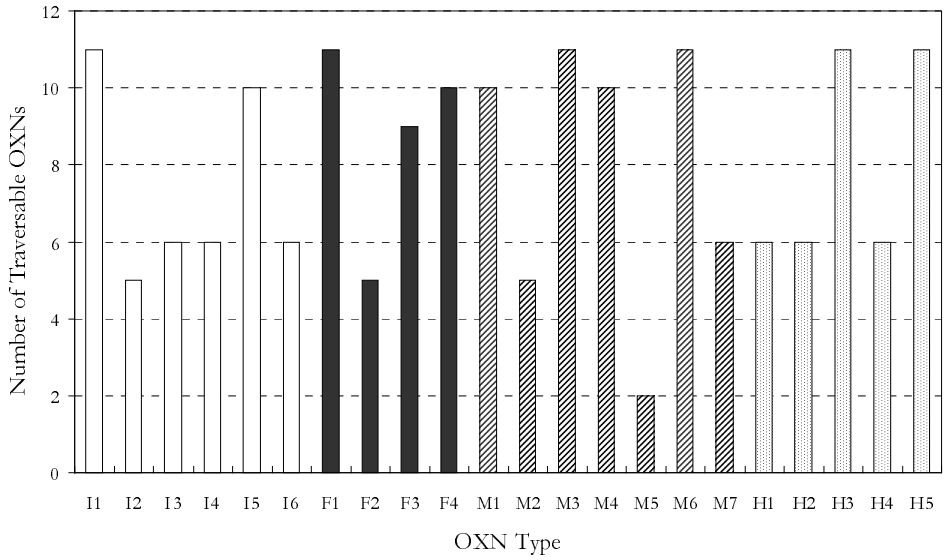


Fig. 5. Number of traversable OXNs assuming a *Q factor* requirement of 15.4 dB.

Therefore meshed optical networks with a high connectivity and channel counts might favor microoptic or integrated OXNs because of their relatively efficient scalability characteristics. Techniques for improving OXN scaleability have been proposed, this includes wavelength granularity (grouping wavelength channels with similar destinations [48]) and multistage OXN configurations [7].

## 6. Summary

We have analyzed the upper bound on the optical hop count for DWDM meshed transport networks (e.g. ASON) for various classes of OXNs. The information obtained is useful for the OXN selection in the network planning or upgrade stage and application of constraints on the RWA algorithms. Of the fundamental OXNs analyzed, microoptic and all-fiber OXNs demonstrated the overall best cascadability performance. However, it was noted that the influence of the configuration of OXNs increases when considering OXNs with a large $\Delta$ or when tightly packed channels (large $N_\lambda$) have to be cross-connected. This suggests that integrated or microoptic OXNs are better equipped to relax the upper bound on $H$. Furthermore, the limits on $H$ observed can also be used to offer guidelines on the implementation of DWDM SPRINGs since their OADMs are essentially 2×2 OXNs. This is of great importance since DWDM SPRINGs are generally considered to the next step in the evolution of the current legacy networks.

#35114 - $15.00 US Received August 29, 2001; Revised September 28, 2001